Am J Cancer Res 2021;11(11):5338-5357
www.ajcr.us /ISSN:2156-6976/ajcr0136527

Original Article

YYFZBJS inhibits colorectal tumorigenesis by remodeling gut microbiota and influence on M2 macrophage polarization *in vivo* and *in vitro*

Ni Chai[1*], Yibai Xiong[2*], Yuli Zhang[3,4*], Yuelei Cheng[5], Wenfei Shi[6], Yiqing Yao[1], Hua Sui[3], Huirong Zhu[7]

[1]Oncology Department, Yueyang Hospital of Integrated of Traditional Chinese and Western Medicine, Shanghai University of Traditional Chinese Medicine, Shanghai 200437, China; [2]Institute of Basic Research in Clinical Medicine, China Academy of Chinese Medical Sciences, Beijing 100700, China; [3]Medical Experiment Center, Jiading Branch of Shanghai General Hospital, Shanghai Jiao Tong University School of Medicine, Shanghai 201803, China; [4]Department of Traditional Chinese Medicine, Jiading Branch of Shanghai General Hospital, Shanghai Jiao Tong University School of Medicine, Shanghai 201803, China; [5]Department of Medical Oncology, Shuguang Hospital, Shanghai University of Traditional Chinese Medicine, Shanghai 201203, China; [6]Oncology Department, Shanghai Municipal Hospital of Traditional Chinese Medicine, Shanghai University of Traditional Chinese Medicine, Shanghai 200271, China; [7]Shanghai University of Traditional Chinese Medicine, Shanghai 201203, China. [*]Equal contributors.

Received June 19, 2021; Accepted September 7, 2021; Epub November 15, 2021; Published November 30, 2021

Abstract: Our previous studies indicated that the extract of Yi-Yi-Fu-Zi-Bai-Jiang-San (YYFZBJS) had potent anticancer activities by significantly inhibiting intestinal tumor development in $Apc^{Min/+}$ mice. However, knowledge regarding the mechanism and effect of YYFZBJS in the prevention of colorectal cancer is limited. In this study, we aim to investigate the preventive effects of YYFZBJS in *enterotoxigenic Bacteroides fragilis* (ETBF)-colonized mice with azoxymethane (AOM)/dextran sulfate sodium (DSS)-induced tumorigenesis. First, the colonic tissues of the AOM/DSS mouse models were collected for biomedical analysis, and gut microbiota profiling was detected post YYFZBJS treatment using a 16S rRNA gene sequencing. Then, antibiotic solution (Abx) mice were acclimated with AOM/DSS treatment and then fed with ETBF with or without YYFZBJS for three cycles. As expected, the intragastric administration of YYFZBJS in the AOM/DSS mouse model significantly decreased the tumor load, the severity of disease activity index (DAI) scores, and the level of M2 macrophage markers such as CD206, Arg-1 and IL-10. Notably, the reverse of polarized macrophages induced by YYFZBJS could suppress CRC cell proliferation and infiltration, as demonstrated by the decrease of some tumor proliferation-related proteins in a dose-dependent manner. Importantly, ETBF dysbiosis can contribute to colon tumor development by stimulating p-STAT3 mediated M2 macrophages polarization to promote chronic inflammation and adenoma malignant transformation, which YYFZBJS can effectively limit. Altogether, we demonstrate that ETBF dysbiosis may contribute to M2 macrophages-promoted colon carcinogenesis and progression of CRC cells, while YYFZBJS could be a promising protective agent against ETBF-mediated colorectal cancer.

Keywords: Colorectal cancer, ETBF, AOM/DSS-induced colitis-associated colorectal cancer, macrophage, signal pathway

Introduction

The recent rapid increase in colorectal cancer (CRC) incidence is a severe health problem worldwide, as it possesses one of the highest rates of cancer-related mortality [1]. Colorectal cancer usually develops from adenomatous polyps (adenoma) that undergo dysplastic changes to become cancerous (adenocarcinoma) [2]. However, the development of CRC remains to be understood entirely owing to its complexity. Recently, accumulating evidence suggested that the gut microbiota, chronic inflammation, host genetic predisposition, and environmental factors are linked with the progression of CRC [3, 4]. Others and our data demonstrated that enterotoxigenic Bacteroides fragilis (ETBF) strains could secrete the B.

fragilis toxin to promote tumor growth by mediating tumor immune escape [5, 6].

Additionally, accumulating evidence has shown that the activity of ETBF is significantly higher in individuals with spontaneous CRC and individuals from familial adenomatous polyposis families [7-9]. Moreover, a series of studies have demonstrated that Treg expansion in the colonic lamina propria lymphocytes (LPL) of ETBF-colonized *Apc*$^{Min/+}$ mice is driven by tissue-resident macrophages [10, 11].

Moreover, these and other studies, including those from our laboratory, revealed an equally critical role for T-regulatory cells (Treg) in driving tumor growth in the ETBF-colonized gut [12, 13]. Usually, *Apc*$^{Min/+}$ mice are often utilized to elucidate mechanisms of intestinal tumorigenesis *in vivo.* However, the carcinogen-induced azoxymethane/dextran sulfate sodium (AOM/DSS) mouse model of colon cancer is also widely used to investigate the roles of dietary factors in tumor development and malignant evolution in the colon [14, 15]. In the current study, we assessed the tumorigenic potential of ETBF colonization in the germ-free (GF) mediated AOM/DSS mouse model. We found that ETBF colonization in GF mice administered with AOM/DSS resulted in the rapid development of a large number of polyps predominantly in the colorectal region compared with wild-type GF mice.

In the tumor microenvironment, tumor-secreted chemokines and growth factors could induce monocytes' recruitment and differentiation to macrophages [16]. With the influence of those cytokines' signals, TAMs (tumor-associated macrophages) undergo polarization into M1 and M2 phenotypes, promoting tumor metastasis [17]. The primary M2 markers include CD206, Arg-1, IL-10, and TGF-β. The primary M1 markers include CD11b, iNOS, IL-12, and TNF-α [18]. Increasing evidence has shown that the high density of M2 macrophages is related to shorter survival time and a high risk of recurrence in clinical studies [19, 20]. A series of studies further confirmed that M2 macrophages play an essential role in promoting CRC growth and invasion [21]. Similarly, we also confirmed the critical role of M2 macrophages in promoting the occurrence of intestinal tumors in the AOM/DSS mouse model [17].

The results of those studies suggest that the modulation of the microbiota might be a good strategy to prevent or cure CRC and that uncovering how symbionts suppress inflammatory response warrants further investigation [22]. Clearance of ETBF by cefoxitin, a semi-synthetic and broad-spectrum cephalosporin antibiotic, inhibited ETBF-promoted tumorigenesis in multiple intestinal neoplasia mice [23]. However, to this date, no studies have investigated the suppressive effects of natural products or Traditional Chinese Medicine (TCM) on ETBF-mediated tumorigenesis in mice. Previous research has demonstrated the health-promoting properties of various dietary natural compounds, including carotenoids, flavonoids, and polyphenols obtained from vegetables and fruits [24]. However, few chemotherapeutic drugs are available, and such drugs have significant toxic side effects that can severely impair the immune system and hematopoietic system [26, 27]. Our previous studies have shown that the fecal microbiota transplantation (FMT) from Yi-Yi-Fu-Zi-Bai-Jiang-San (YYFZBJS) volunteers altered dysregulated inflammation and oncogenic pathways and inhibited intestinal tumorigenesis [5].

Herein, we investigate the effect of YYFZBJS in the carcinogen-induced AOM/DSS mouse model of colon cancer and the ETBF enrichment in the gut microbiota to evaluate the prevention mechanism of ETBF-mediated tumorigenesis. Furthermore, by gavaging germ-free AOM/DSS mice with ETBF strains, we demonstrated that ETBF accelerated colonic tumorigenesis development, partly by modulating the polarization of M2 macrophages. Furthermore, we examined the alteration of M2 macrophages polarization in GF/AOM/DSS mouse tumor tissue after YYFZBJS treatment and the efficacy, and associated mechanisms of the ETBF and YYFZBJS combined effect on intestinal tumor development both *in vitro* and *in vivo*. This will help us better understand the molecular biological mechanism in YYFZBJS and its anticancer effect, contributing to its further application in CRC prevention.

Materials and methods

Cell culture and reagents

Mice colorectal adenocarcinoma MC-38 cells were purchased from the Shanghai Cell Collection (Shanghai, China). Cells were cultured in RPMI 1640 with 10% fetal bovine serum (Gibco, NY, USA), 2 mM glutamine, 100

units/ml streptomycin, and penicillin (Invitrogen, Carlsbad, CA). The cells were grown at 37°C in a humidified 5% CO_2 atmosphere. Bone marrow-derived macrophages (BMDMs) were prepared as previously described [28]. BMDMs were stimulated with IL-4 (100 ng/ml, 48 h) for M2 polarized activation. Monoclonal antibodies specific for JNK (3708), NFκ-B (3036), c-Met (3127), cyclinD1 (4668s), MMP-2 (4668s), MMP-9 (4668s), STAT3 (9139), p-STAT3 (9145s) and GAPDH (5174s) were obtained from Abcam plc (Cambridge, UK) and Cell Signaling Technology Inc. (Boston, MA, USA).

Preparation of Chinese YYFZBJS herb formula

YYFZBJS was formulated by Yi-yi-ren (lot# 18-0103), Fu-Zi (lot# 180709) and Bai-jiang-cao (lot# 180522) in a ratio of 30:6:15. Chinese medicines were purchased from Shanghai Hua Yu Chinese Herbs Co., Ltd. (Shanghai, China) and were processed as described previously [5]. All herbs from YYFZBJS herb formula are authenticated by Pharmacopoeia of the People's Republic of China (2015). Briefly, the mixture (51 g) was extracted twice for 1 h each time by refluxing in ethanol (1:8, v/v). The filtrates were concentrated and dried in a vacuum at 60°C. The concentrated extract was then dried by lyophilization to obtain the YYFZBJS extract at a yield of dried powder of 24.4%. The extract was stored at 4°C, and its preparations were standardized, regulated, and quality controlled according to the guidelines defined by the Chinese State Food and Drug Administration (SFDA). For quality control, the fingerprint spectrum for YYFZBJS was performed by the UHPLC-Q Exactive system as described previously [5].

Induction of AOM-initiated and DSS-promoted colon carcinogenesis

The 6-week-old SPF female C57BL/6J mice were obtained from Shanghai Super-B&K Animal Laboratory Co., Ltd. (Shanghai, China) with Certification No. SCXK 2016-0016. All animals were housed under specific pathogen-free conditions per the provision and general recommendation of the Chinese Experimental Animals Administration Legislation. The procedures used for the induction of the CAC model by AOM and DSS were as previously described [17]. Briefly, on day 1, the mice were injected with AOM (12.5 mg/kg, i.p.). After 1 week, 2.5% DSS (International Lab, Chicago, IL, USA) was added to the drinking water for 7 days, followed by 14 days of tap water for recovery. This cycle was repeated twice. As shown in **Figure 1A**, the intragastric administration of YYFZBJS-L/M/H was given at a dosage of 3.825 g/kg, 7.65 g/kg, and 15.3 g/kg according to HED (human equivalent dose) [5, 29]. YYFZBJS-L/M/H and Aspirin (30 mg/kg) were given orally for 9 weeks during the DSS treatment separately, as previously described [1]. Aspirin was the positive control because it could effectively inhibit intestinal adenomatous polyposis and colon carcinogenesis [5, 17]. The Control group was oral gavaged with the same volume of sterile isotonic saline and fed with normal drinking water.

Mouse strains and breeding

As shown in **Figure 3A**, mice were treated for 4 weeks with an antibiotic solution (Abx) containing Ampicillin (1 mg/ml), Neomycin (1 mg/mL), Metronidazole (1 mg/ml), and Vancomycin (0.5 mg/mL) added to the sterile drinking water, as previously described [5]. After four weeks, Abx treatment was stopped, and the mice were treated with AOM and DSS combined with ETBF (1×10^8 colony forming units) or Vehicle (E. coli MG1655 or the same volume of phosphate buffer saline) every day for the development of neoplastic lesions, as previously described. ETBF was grown under anaerobic conditions at 37°C overnight before administration to mice, as described previously [30]. Signs of illness were monitored daily and body weight was recorded weekly.

Microbial analysis of mouse stool

Feces of all mice in the NS and YYFZBJS groups were collected for gut microbiota analyses. Briefly, (i) genomic DNA was extracted using a Power Soil DNA Isolation Kit (MO BIO Laboratories, Carlsbad, CA); (ii) the 16S rDNA V4 region was amplified using the 515F and 806R primers; (iii) PCR product quantification, qualification, and purification were performed; (iv) library preparation and sequencing were performed on the MiSeq platform (Illumina, Inc., San Diego, CA). The 16S rRNA sequencing data were quality filtered using FLASH (Fast Length Adjustment of Short reads, Version 1.2.11). Operational taxonomic units (OTUs) were picked at a 97% sequence similarity cut-off, and the purified amplicons were

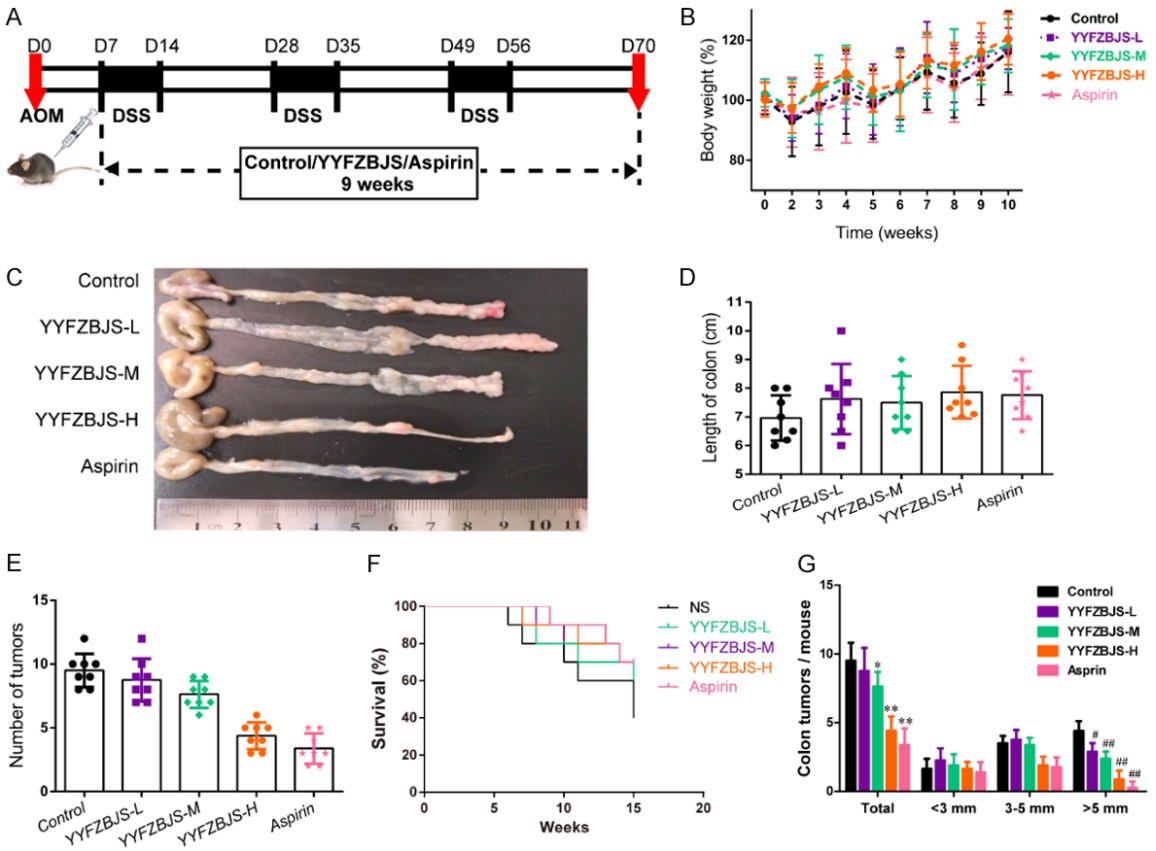

Figure 1. Effect of YYFZBJS on the occurrence and progression of CAC. (A) Experimental protocol used for the induction of the CAC model in C57BL/6J mice. (B, D-F) Effects of the model and treatment on mice body weight (B), colon length (D), number of intestinal polyps (E) and survival (F) in mice. (C) Microscopic view of the colon in mice. (G) The tumor size distribution in the intestine was listed and compared with the control. Data are presented as means ± SD of 8 animals per experimental group, with Welch's correction, two-tailed t-test. $^{\#}P<0.05$, $^{\#\#}P<0.01$; $^{*}P<0.05$, $^{**}P<0.01$ *vs*. control.

sequenced on an Illumina MiSeq platform at Majorbio Bio-pharm Technology Co. Ltd. according to the standard protocols.

Histology and immunohistochemistry

The whole intestine was removed immediately after sacrifice and opened longitudinally after being washed with ice-cold phosphate buffer saline (PBS) as previously described [5]. The number, location, and size of visible tumors throughout the intestine were measured to calculate the incidence of adenoma. Tumor numbers were counted and grouped based on sizes: <3 mm, 3-5 mm, and >5 mm. Tissue sections were fixed in 10% formalin followed by paraffin embedding. Then they were stained with hematoxylin and eosin for pathological evaluation by a pathologist blinded to the experimental groups. Histological analysis for polyp, adenoma and adenocarcinoma was performed by a board-certified pathologist (PV), as previously described [5]. The histology scoring criteria is as follows: 0 = normal, 1 = moderate, 2 = marked and 3 = severe.

For the murine samples, immunohistochemistry was performed to detect total Ki67 (anti-mouse Ki67, Abcam), PCNA (anti-mouse PCNA, Abcam); all stains used horseradish peroxidase-conjugated antibody, with chromogenic detection with the substrate 3-3'-diaminobenzidine, and finally counterstained with hematoxylin.

Cytokine antibody arrays

Serum samples were screened in duplicates using a Mouse Cytokine Array QAM-INF-1 (RayBiotech) containing slides coated with 40 different cytokines according to the manufacturer's guidelines with some modifications as pre-

viously described [5]. Briefly, the arrays were blocked, incubated with 100 mL of condition medium overnight, followed by biotin-conjugated antibodies (1/250) incubation for 2 hr and with HRP-linked secondary antibody (1/1000) for 1 h. The membranes were incubated with a peroxidase substrate, and the results were documented using XAR films. Quantitative array analysis was performed using Array Vision Evaluation 8.0 (GE Healthcare Life Science).

Co-incubation of ETBF and CRC cells

ETBF was grown in Luria-Bertani (LB) broth at 37°C overnight to mid-log phase. The concentration of bacteria was adjusted based on the optical density reading at 600 nm analyzed by NanoDrop ND-2000. Bacteria were diluted to 1:10 with a suitable medium before co-culture with macrophages and CRC cells [30]. Briefly, MC-38 cells w/o treatment of IL-4-primed macrophage RAW264.7 cells were seeded into 6-well lumox plates (Vivascience, Gloucestershire, UK) and grown to 70% confluence before co-culture with ETBF at 10^6 CFU/ml in RPMI-1640 supplemented with 10% fetal bovine serum for 6 h. ETBF was allowed to infect the monolayers of CRC cells. All extracellular bacteria were killed by gentamicin (500 μg/ml for 20 min), and the dead bacteria were removed by extensive washing with PBS [31].

RNA-seq and analysis

Total RNAs from CRC cells were isolated with trizol and the RNA-seq library was prepared by the lcsciences Co. Ltd. RNA-Seq FASTQ files were processed using the RNA-Seq module implemented in the CLC Genomics Workbench v8.0 software (Qiagen Bioinformatics) with default settings, as previously reported [32]. Reads counts were normalized based on RPKM (Fragments Per Kilobase per Million mapped reads). Heatmaps were drawn using multiple array viewer.

Western blot and immunofluorescence analysis

Whole-cell lysates were prepared for the Western blot analysis of Arg-1, iNOS, p-JNK, p-STAT3, p-ERK, and GAPDH expression as previously reported [33]. Briefly, the cells were maintained on ice in a lysis buffer for 2 h before being collected with a cell scraper. The sample was centrifuged, and the supernatant was collected and stored at -80°C until use. A densitometric analysis was performed using the Scion Imaging application (Scion Corporation), and GAPDH was used as an internal reference.

Immunofluorescence analyses in RAW264.7 cells were incubated with rabbit anti-Arg-1 primary antibody (Bioss Antibodies) prepared in blocking solution (10% horse serum, 0.1% Triton X-100, 0.02% sodium azide, PBS) followed by incubation with a fluorescent dye-conjugated donkey anti-rabbit secondary antibody (Molecular Probes). DAPI (4-,6-diamidino-2-phenylindole) (Life Technologies) staining was performed following the manufacturer's protocol, and fluorescence images were obtained using a Diaphot 300 fluorescence microscope (Nikon) with SPOT software (Sterling Heights) as previously described [34].

Flow cytometry

Phenotype analysis of the macrophages was performed with a BD FACS AriaII flow cytometer (BD, USA) as previously described [17]. Briefly, the cells were labeled with CD11b-FITC, F4/80-PE, and CD206-APC (eBioscience, San Diego, CA) following the manufacturer's protocol. To analyze the prevalence of M2 macrophages, the cells were incubated with PE-conjugated F4/80 antibodies or APC-conjugated CD206. Flow cytometry was performed using a FACS CaliburTM flow cytometer, and the data were analyzed using Paint-A-Gate software (Becton Dickinson).

Analysis of cytokine expression in mouse tumor

The mouse tumor samples were analyzed to detect mouse cytokines by ELISA according to the manufacturer's instructions (eBioscience) and as previously described [5].

Cell viability assays

Cell proliferation was determined using the CCK-8 cell counting kit (Sigma-Aldrich). Briefly, CRC cells were seeded in 96-well plates at 1×10^4 cells/well after co-culture. The CCK-8 assay was performed 48 h after treatment. Treated cells were incubated for 4 h with a culture medium containing the CCK-8 reagent,

absorbance was measured at 450 nm using a microplate enzyme-linked immunosorbent assay reader (Labsystems Dragon, Wellscan). The relative survival rate of cell growth was calculated and presented as previously described [17]. All experiments were conducted using 5 wells per experiment and repeated at least three times independently.

Transwell co-culture assay

MC-38 cells and BMDMs were co-cultured with BMDMs ETBF at 10^6 CFU/ml for 6 h as described above. For the cell proliferation assay, the inserts were placed in a 24-well plate with pre-seeded TAMs. Then, cancer cell activity was detected using the trypan blue method. For the cell invasion ability assay, TAMs were seeded on the bottom of a 24-well plate with cancer cells in a Transwell chamber such that both cell populations were exposed to the same conditions.

Statistical analysis

All the numerical data were presented as means ± standard deviation. All statistical analyses were performed using GraphPad Prism 6 (GraphPad Software) and SPSS 18.0 (Chicago, IL, USA). A two-sided unpaired Student's t-test with Benjamini-Hochberg correction was used to compare two groups. The differences among the several groups were analyzed using one-way variance (ANOVA) analysis followed by Duncan's test. They were used to analyze colon tumor numbers, IHC, Western blot, Elisa, cell viability, quantitative RT-PCR, and transwell migration. The Wilcoxon rank-sum test was used for gut microbiome analysis of mice. Data are presented as three independent experiments at least. Significant probability values were indicated as $^{*}P<0.05$, $^{**}P<0.01$; $^{\#}P<0.05$, $^{\#\#}P<0.01$.

Results

YYFZBJS suppresses colorectal tumorigenesis in the CAC mouse model

Previously, we showed that YYFZBJS alone was sufficient to inhibit intestinal tumorigenesis in $Apc^{Min/+}$ mice. In the present study, to investigate the preventive effects of YYFZBJS on CAC formation, murine treatment was initiated at the age of 6 weeks. The workflow of the animal experiment in anti-tumorigenesis effect of YYFZBJS is depicted in **Figure 1A**. After the AOM/DSS treatment, the significant body weight loss (**Figure 1B**) was lessened following the addition of YYFZBJS in a dose-dependent manner.

In addition, YYFZBJS decreased the colon adenoma incidence and tumor number by 7.89%, 19.74% and 53.95%, respectively, in a dose-dependent manner (**Figure 1C**, **1E**). As shown in **Figure 1D** and Table S1, compared to the AOM/DSS-treated group, the mice treated with YYFZBJS or Aspirin showed a bodyweight recovery. **Figure 1F** shows that the administration of YYFZBJS significantly increased the survival rate of the mice compared with that of the mice in the NS group (Control), which received an equivalent volume (μL) of normal saline. Notably, the numbers of polyps in all three YYFZBJS groups were much fewer than that of the non-treated control group (**Figure 1G**). These results suggest that YYFZBJS is effective in protecting against AOM/DSS-induced colitis-associated tumorigenesis.

YYFZBJS modulates the gut microbiome composition in the CAC mouse model

To investigate if the colon protective effect of YYFZBJS is, at least in part, we performed 16S rRNA sequencing to detect the influence of YYFZBJS on the microbiota composition in the AOM-initiated and DSS-promoted colon carcinogenesis mouse model. We compared the gut microbiota between YYFZBJS and Control group through linear discriminant analysis effect size (LEfSe) to identify the specific microbiota linked to the colon carcinogenesis model. Dubosiella, Clostridium and Bacillus, whose members are generally associated with butyrate production, were more abundant in the YYFZBJS group (**Figure 2A**). Both Chao and Shannon indexes did not change significantly in the four groups, indicating that YYFZBJS treatment could not alter the OTU number of gut microbiota (**Figure 2B**). However, the Simpson index showed significant change between the YYFZBJS and the control groups, suggesting that YYFZBJS had a stronger positive effects on the α diversity of the gut microbiota (**Figure 2B**). Four major phyla dominated the gut microbiota of all the samples: Bacteroidetes, Ruminococcaceae, Lactobacillus, and Muribaculaceae (data not shown). The genus-level analysis revealed that YYFZBJS increa-

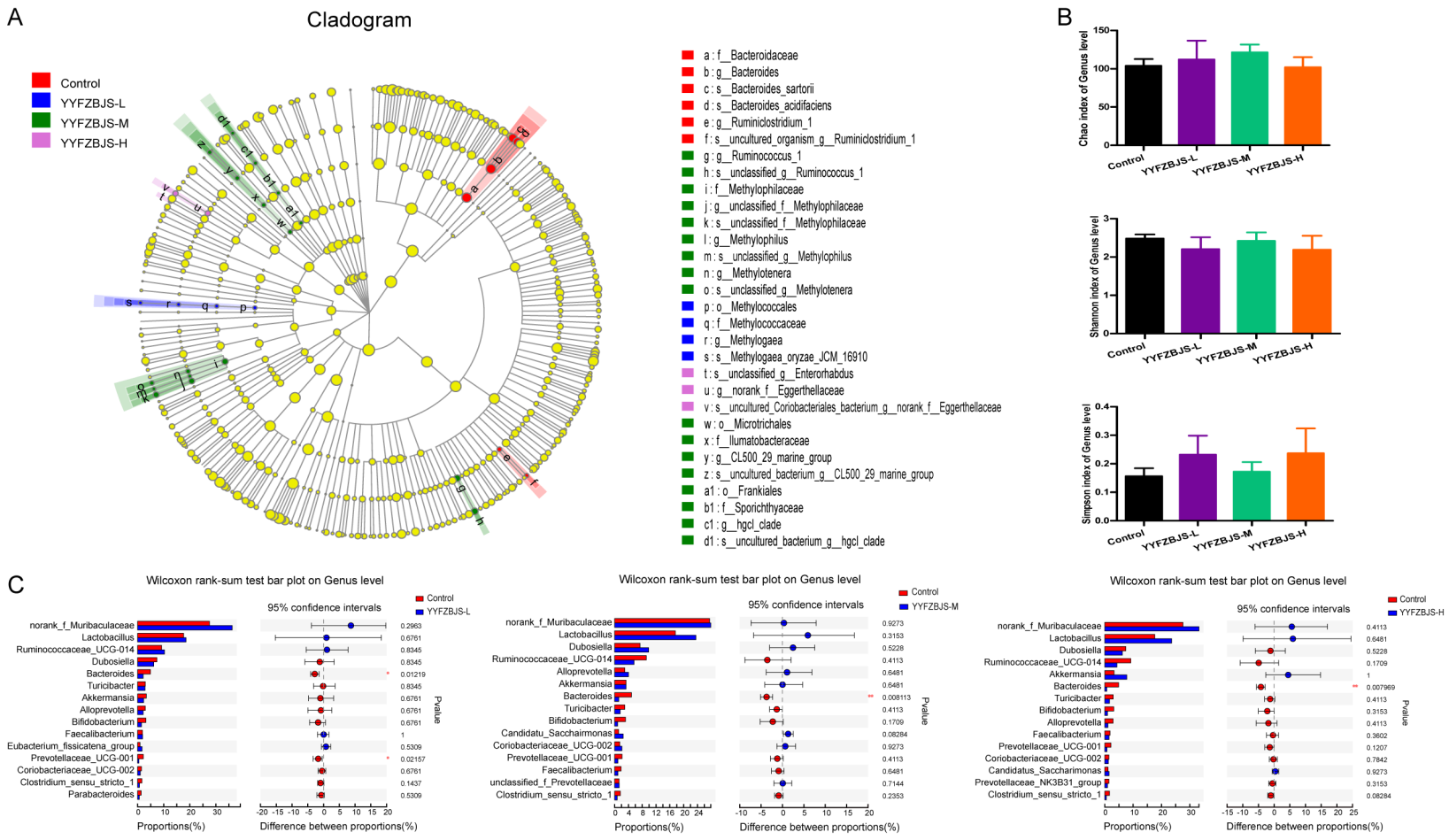
A
Cladogram
Control
YYFZBJS-L
YYFZBJS-M
YYFZBJS-H
a : f__Bacteroidaceae
b : g__Bacteroides
c : s__Bacteroides_sartorii
d : s__Bacteroides_acidifaciens
e : g__Ruminiclostridium_1
f : s__uncultured_organism_g__Ruminiclostridium_1
g : g__Ruminococcus_1
h : s__unclassified_g__Ruminococcus_1
i : f__Methylophilaceae
j : g__unclassified_f__Methylophilaceae
k : s__unclassified_f__Methylophilaceae
l : g__Methylophilus
m : s__unclassified_g__Methylophilus
n : g__Methylotenera
o : s__unclassified_g__Methylotenera
p : o__Methylococcales
q : f__Methylococcaceae
r : g__Methylogaea
s : s__Methylogaea_oryzae_JCM_16910
t : s__unclassified_g__Enterorhabdus
u : g__norank_f__Eggerthellaceae
v : s__uncultured_Coriobacteriales_bacterium_g__norank_f__Eggerthellaceae
w : o__Microtrichales
x : f__Ilumatobacteraceae
y : g__CL500_29_marine_group
z : s__uncultured_bacterium_g__CL500_29_marine_group
a1 : o__Frankiales
b1 : f__Sporichthyaceae
c1 : g__hgcl_clade
d1 : s__uncultured_bacterium_g__hgcl_clade
B
Chao index of Genus level
Shannon index of Genus level
Simpson index of Genus level
Control
YYFZBJS-L
YYFZBJS-M
YYFZBJS-H
C
Wilcoxon rank-sum test bar plot on Genus level
95% confidence intervals
Proportions(%)
Difference between proportions(%)
Pvalue
norank_f_Muribaculaceae
Lactobacillus
Ruminococcaceae_UCG-014
Dubosiella
Bacteroides
Turicibacter
Akkermansia
Alloprevotella
Bifidobacterium
Faecalibacterium
Eubacterium_fissicatena_group
Prevotellaceae_UCG-001
Coriobacteriaceae_UCG-002
Clostridium_sensu_stricto_1
Parabacteroides
Candidatu_Sacchairmonas
Coriobacteriaceae_UCG-002
unclassified_f_Prevotellaceae
Candidatus_Saccharimonas
Prevotellaceae_NK3B31_group

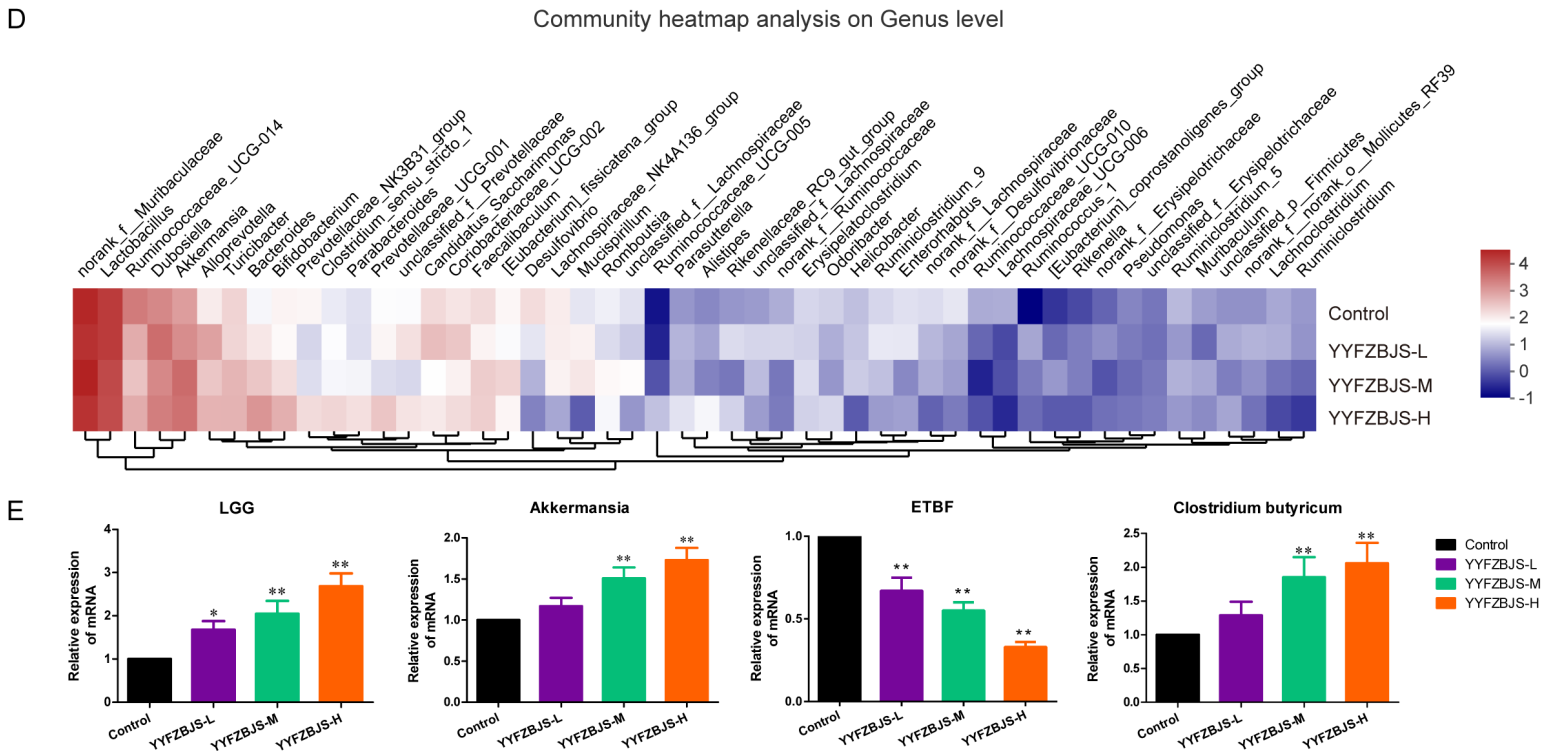

Figure 2. YYFZBJS modulated the composition of the gut microbiota in AOM/DSS mice. A. Cladogram generated from the linear discriminant analysis effect size (LEfSe) between YYFZBJS group and Control group (n = 8 for each group). The analyses were performed at the end of the experiment. B. α Diversity of gut microbiota for mice in four different groups. C. Bar plot of compositional differences at the genus level in the gut microbiome of mice in the combination YYFZBJS group vs. the control group by the Wilcoxon rank-sum test. Data are expressed as mean ± SD. $^{*}0.01<P\leq0.05$, $^{**}0.001<P\leq0.01$, $^{***}P\leq0.001$, Two-sided Hypotheses. D. Heat map of the genus with relative abundances significantly different from their relative abundances at the time of YYFZBJS administration. The differentially enriched bacterial genus in C57BL/6J mice receiving N.S and YYFZBJS. The relative abundance between control and treatment mice for the genus was calculated for each time point. E. Gut microbiota level was analyzed for mRNA expression of Lactobacillus rhamnosus (LGG), Akkermansia, ETBF, and Clostridium butyricum by quantitative RT-PCR. Data are presented as means ± SD of 8 animals per experimental group, with Welch's correction, two-tailed t-test. $^{*}P<0.05$, $^{**}P<0.01$, *vs*. Control.

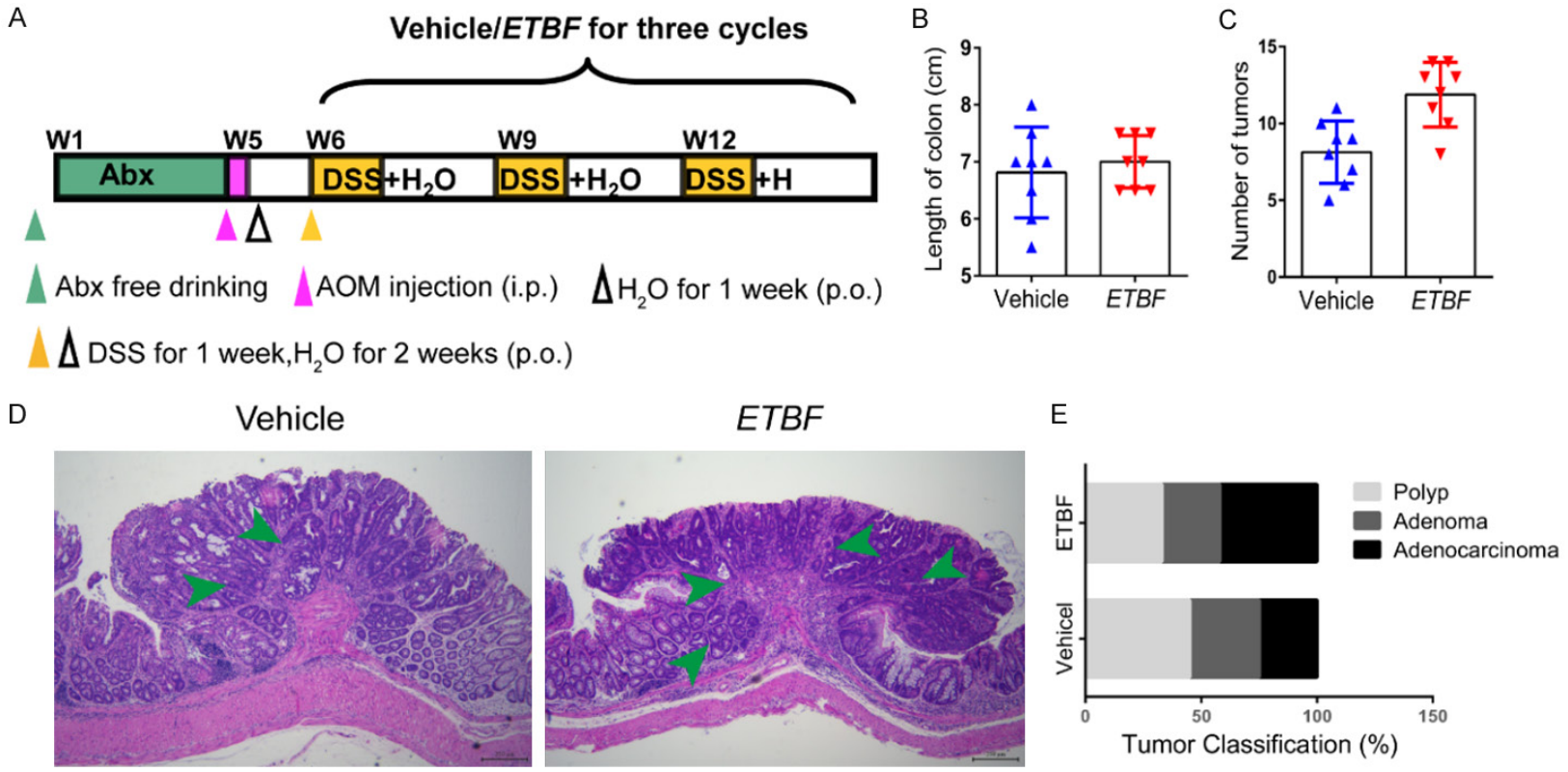
A
Vehicle/ETBF for three cycles
W1
W5
W6
W9
W12
Abx
DSS+H2O
DSS+H2O
DSS+H
Abx free drinking
AOM injection (i.p.)
H2O for 1 week (p.o.)
DSS for 1 week,H2O for 2 weeks (p.o.)
B
Length of colon (cm)
Vehicle
ETBF
C
Number of tumors
Vehicle
ETBF
D
Vehicle
ETBF
E
ETBF
Vehicel
Polyp
Adenoma
Adenocarcinoma
0
50
100
150
Tumor Classification (%)

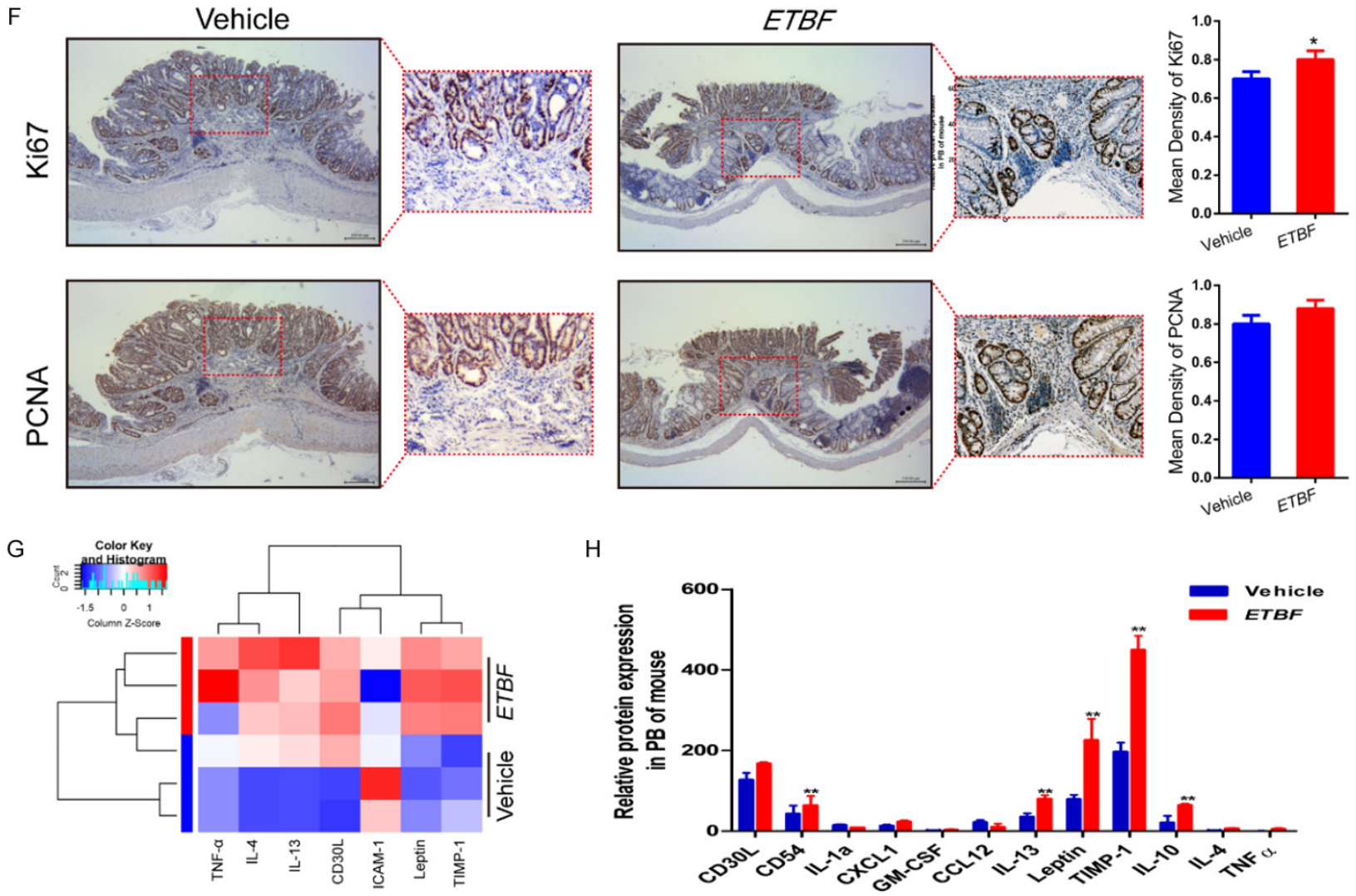

Figure 3. ETBF infection enhances colonic tumorigenesis and reduces the inflammatory response in the AOM/DSS mouse model. (A) Experimental design indicating the timing of the intragastric administration and organization of groups. Mice were treated with Abx from W1 (age at week 4) to W4, then injected with AOM (12.5 mg/kg, i.p.) and provided drinking water for 1 week, and three cycles of DSS and drinking water for 3 weeks as described in the Methods section. During the treatment, ETBF and Vehicle were orally administered at a dosage of 10^8 CFU/mice. (B, C) Effects of ETBF on colon length (B) and the number of tumors (C) in the GF/AOM/DSS mouse model. (D) Typical adenomatous intestinal polyp with an early invasion of neoplastic glands into the muscular layers was often observed in ETBF infected GF/AOM/DSS mice. This typical regressive intestinal cancer morphology is observed throughout the intestine in the mice. Blue arrows indicated adenocar-

cinoma cells. Magnification bars, 100 μM. (E) Histology evaluation of colon tumors: quantitatively represented as polyp, adenoma, and adenocarcinoma. (F) Immunohistochemical staining using an antibody against Ki67 and PCNA in the vehicle group and ETBF infection group. Magnification bars, 100 μM. Data are presented as the means ± SD of 5 regions per slice with Welch's correction, two-tailed t-test. $^{**}P<0.05$, *vs*. Vehicle. (G) The difference between the two groups in inflammatory cytokines as assessed by cytokine antibody array. (H) The mRNA expression levels of inflammatory factors, such as IL-12, TNF-α, and IL-10 in the PB of mice in different groups. The data are presented as the mean ± SD from at least three experiments. $^{**}P<0.01$ *vs*. Vehicle.

sed the relative abundance of pathogenic bacteria, such as Lactobacillus, Ruminococcaceae, and Clostridium (**Figure 2C**, **2D**). Notably, compared with the control, a lower mRNA expression of *enterotoxigenic Bacteroides fragilis* (ETBF) was observed in different doses of YYFZBJS treatment mice (**Figure 2E**). Additionally, a relative up-regulation of Lactobacillus rhamnosus (LGG) and Clostridium butyricum was observed in mice fed with YYFZBJS compared with that of the control, and this effect showed a dose-dependent trend with the qPCR analysis mentioned in the Supplementary Material (**Figure 2E** and Table S2).

ETBF infection enhances colonic tumorigenesis and reduces inflammatory responses in the CAC mouse model

Previously, we confirmed the effect of YYFZBJS on the inhibition of tumor development in AOM/DSS mice. A large number of studies have confirmed that ETBF can accelerate tumor occurrence and malignancy. To investigate the mechanism of ETBF in carcinogenesis, germ-free (Abx) mice with AOM and DSS were used as a germ-free (GF) model. The experimental design and timeline are shown in **Figure 3A**. Consistent with the previous results, no difference was noted in the colon length among the treatment groups during the experiment (**Figure 3B**), but the numbers of polyps in ETBF groups were greater than those in the non-treated control group (**Figure 3C**). Similarly, compared to the AOM/DSS-treated group, ETBF increased the colon adenoma incidence and tumor number by 12% and 31.58%, respectively (**Figure 3D**, **3E**). Since Ki67 and PCNA are cell proliferation markers, we examined the localization and expression levels of Ki67 and PCNA by immunohistochemistry in the tumors from the AOM/DSS mice with or without the ETBF treatment (**Figure 3F**).

Emerging studies have found that the promotion effect of ETBF in the development of tumorigenesis is mainly related to the tumor microenvironment [2, 10]. To investigate the mechanism of ETBF in colorectal tumorigenesis, we utilized a cytokine antibody array (Ray Biotech), which demonstrated that compared to the Vehicle group, the ETBF treated mice secreted lower levels of inflammatory cytokines/chemokines, including IL-4, IL-13, and TNF-α, to name a few (**Figure 3G**). We found that the ETBF strains dramatically increased protein expression levels of M2 (IL-4, IL-10, IL-13, etc.) and decreased the levels of ICAM-1, IL-1β, and so on, which are present in the M2 macrophages (**Figure 3H**).

Effect of ETBF on CRC cells through TAMs in vitro

To determine whether the presence of gut commensal bacteria affects regulatory CRC cells and macrophage in vitro, ETBF was co-incubated with MC-38 cells with RAW264.7 macrophages in a Transwell system in which the macrophages were located in the chamber, and the cancer cells were located on the cell plate (**Figure 4A**). The heatmap displays relative fold changes in expression levels of proliferation markers of cancer cells and stem cells in the MC-38 alone group, macrophages co-cultured with MC-38 cells group, and ETBF incubated macrophages with MC-38 cells group (**Figure 4B**).

To explore underlying mechanisms of these ETBF incubated macrophages phenomena on CRC cells, we placed MC-38 cells in a Transwell system and co-cultured with RAW264.7 cells which pretreatment with ETBF for 6 h as described in Method (**Figure 4C**). Interestingly, the protein expression of JNK, STAT3 and NFκ-B were up-regulated in ETBF incubated macrophages and CRC cells compared with that not exposed to the ETBF system (**Figure 4D**). Consistent with western blot results, the effect of ETBF on M2 polarization was verified by the increased Arg-1 aggregation in our IHC analysis (**Figure 4E**).

YYFZBJS inhibited ETBF-induced colorectal tumor development in the CAC mouse model

To further investigate whether regulating the microbiota composition contributed to the protective effect of ETBF, we co-housed the GF/

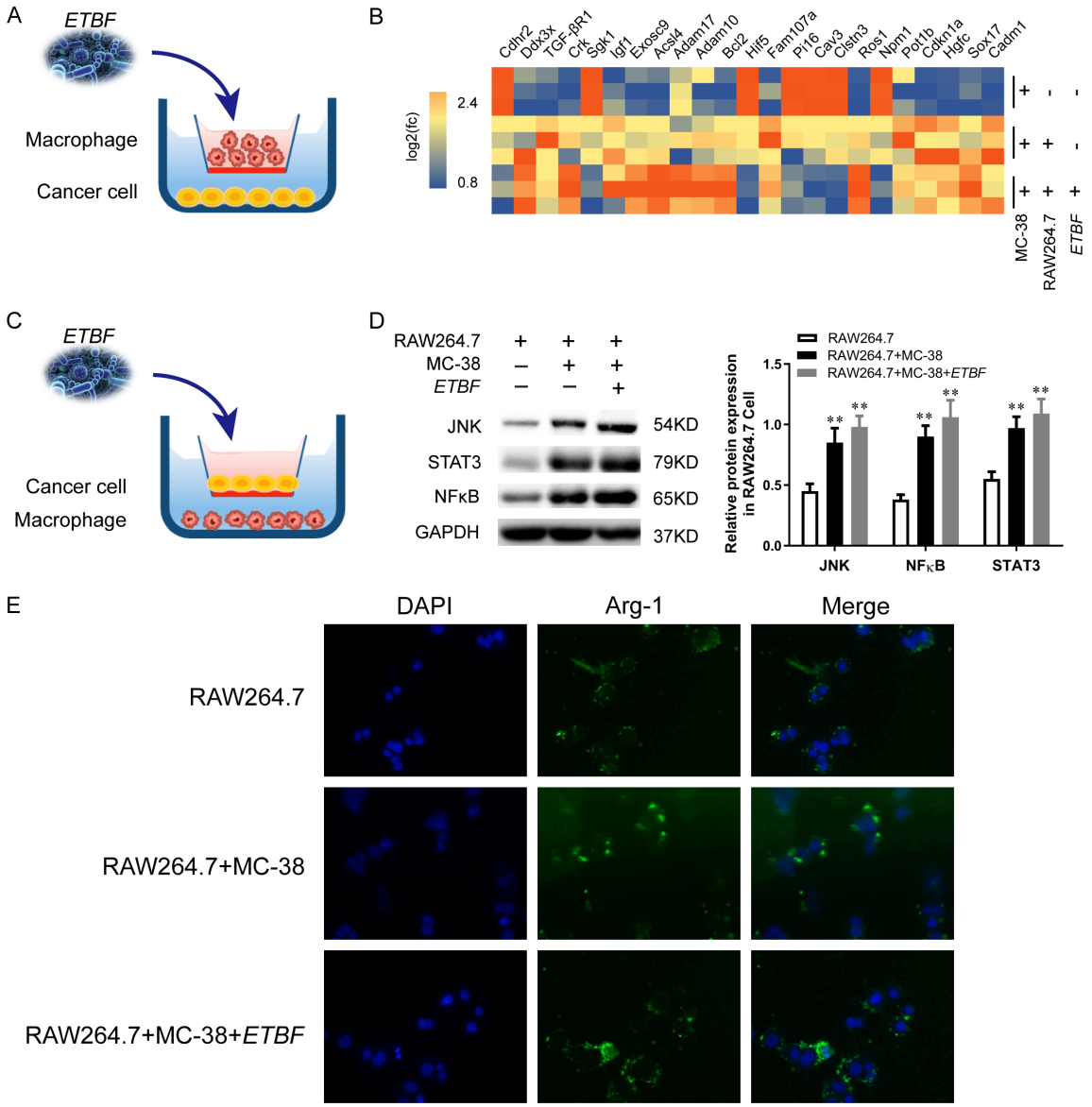

Figure 4. Effect of ETBF on CRC cells through TAMs *in vitro*. (A) After TAMs were co-cultured with MC-38 cells, ETBF was added into the mixture for 6 h. The ratio of cell to bacterial was 1:10. (B) The mRNA of MC-38 cells at the bottom of the cell plate was analyzed by RNA-seq as described in the Methods section. (C) Experimental flow chart of (A). (D) Western blot analysis of JNK, NFκ-B and STAT3 expression in RAW 264.7 cells after infection with ETBF and co-culture with MC-38 cells. Quantifications of migrated cells from three independent experiments are shown as the mean ± S.D. $^{*}P<0.05$, $^{**}P<0.01$, *vs*. RAW 264.7 cells. (E) Immunohistochemical staining with an antibody against Arg-1 in the different groups. Scale bars, 100 μM.

AOM/DSS-treated mice which received ETBF and ETBF plus YYFZBJS to test if the protective effect of YYFZBJS could be counteracted by gut microbiota transmission. We experimented, as shown in Figure S1. We found that ETBF combined with YYFZBJS dramatically decreased polyp numbers in the GF/AOM/DSS model compared to mice given ETBF strains only (**Figure 5A**, **5B**). Moreover, the colon length did not change significantly with or without YYFZBJS, indicating that YYFZBJS treatment does not alter the colon length of GF/AOM/DSS mice infected with ETBF (**Figure 5B**). However, similarly to in vitro results, the expression levels of the STAT3 were significantly decreased in the ETBF plus YYFZBJS group

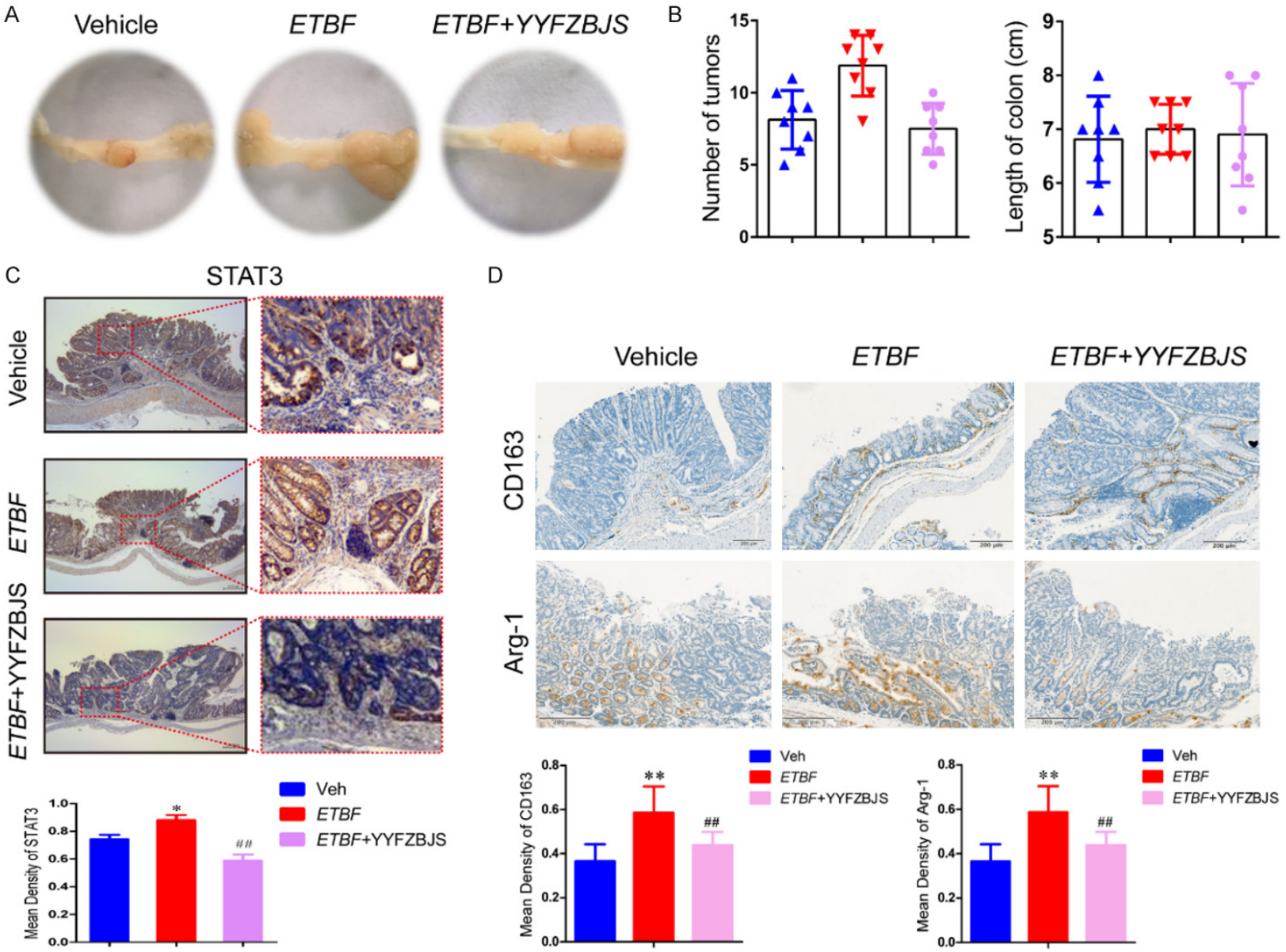
A
Vehicle
ETBF
ETBF+YYFZBJS
B
Number of tumors
Length of colon (cm)
C
STAT3
Vehicle
ETBF
ETBF+YYFZBJS
Mean Density of STAT3
Veh
ETBF
ETBF+YYFZBJS
D
Vehicle
ETBF
ETBF+YYFZBJS
CD163
Arg-1
Mean Density of CD163
Mean Density of Arg-1
Veh
ETBF
ETBF+YYFZBJS

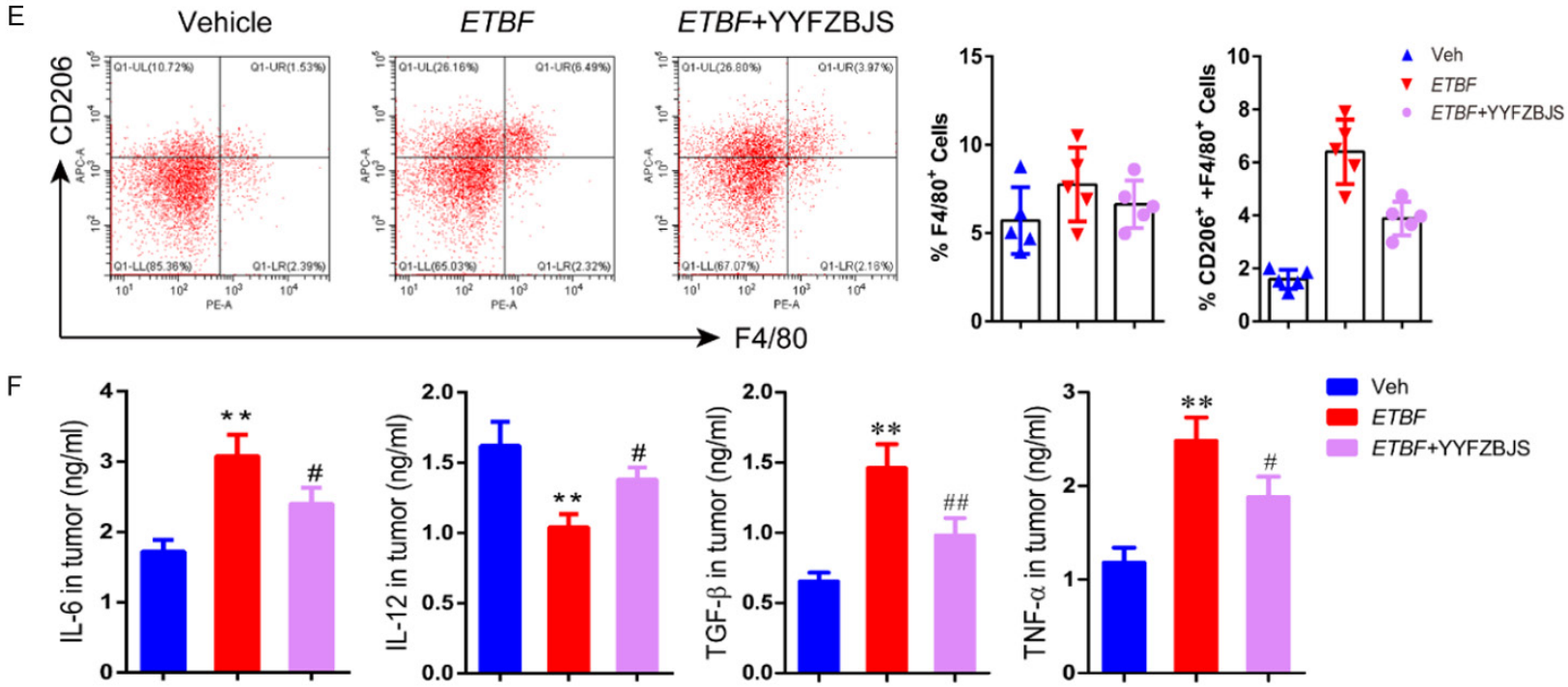

Figure 5. YYFZBJS inhibited ETBF-induced colorectal tumor development in AOM/DSS model. A. Macroscopic view of the representative mouse large intestinal shows several polypoid and discoid colonic tumors from different groups of ETBF-infected mice administered with or without YYFZBJS as shown in Figure S1. GF/AOM/DSS mice were infected with ETBF. During ETBF infection, the YYFZBJS-treated group was orally gavaged with YYFZBJS (15.3 g/kg, p.o., once a day). B. Tumors number and colon length distribution. C, D. Immunohistochemical staining with an antibody against STAT3, CD163, and Arg-1 among Vehicle group, ETBF group and ETBF+YYFZBJS group. Magnification bars, 100 μM. Data are presented as the means ± SD of 8 animals per experimental group with Welch's correction two-tailed t-test. $^{*}P<0.05$, $^{**}P<0.01$, *vs*. Vehicle; $^{\#}P<0.05$, $^{\#\#}P<0.01$, *vs*. ETBF group. E. Representative gating strategy used to identify pulmonary macrophage subsets from intestinal tumor tissue in the GF/AOM/DSS mouse model is shown. Macrophages were analyzed using flow cytometry analysis of the M2 macrophage marker CD206 in the F4/80^{+} cell fraction. The data are presented as the mean ± SD of at least three independent experiments. F. IL-6, IL-12, TGF-β, and TNF-α levels in Tumor were evaluated using ELISA. The data are presented as the mean ± SD of at least three experiments. $^{*}P<0.05$, $^{**}P<0.01$, Vehicle *vs*. ETBF; $^{\#}P<0.05$, $^{\#\#}P<0.01$, Vehicle *vs*. ETBF+YYFZBJS.

compared to the ETBF group (**Figure 5C**). Furthermore, the ETBF plus YYFZBJS-treated GF/AOM/DSS mice demonstrated decreased CD163 and Arg-1 immunoreactivity compared to the ETBF alone mice (**Figure 5D**). Remarkably, after ETBF and YYFZBJS combination feeding, the GF/AOM/DSS mice showed a significant change in M2 polarization, reflected by a reduction in CD206 in the tumor tissue (**Figure 5E**). These data support the role of ETBF combined with YYFZBJS in the process of inflammation during intestinal tumorigenesis. IL-12, TNF-α, and IL-6 are responsible for inducing the M1 phenotype, while IL-4, IL-10, and TGF-β are M2-polarizing cytokines. We found that the secretion levels of the M1-related gene expression of IL-12 and TNF-α were significantly higher, and the IL-10 and TGF-β levels were significantly lower in the colon of the ETBF combined with YYFZBJS mice compared with those in the GF/AOM/DSS mice treated with ETBF only (**Figure 5F**).

YYFZBJS inhibited tumor cell proliferation by regulating ETBF primed BMDMs in vitro

To determine whether the presence of YYFZBJS affects macrophages in vitro, MC-38 cells were co-incubated with M2 macrophages isolated from the BMDMs of YYFZBJS group mice (**Figure 6A**). As shown in **Figure 6B**, CRC cells incubated with YYFZBJS-primed BMDMs displayed significantly lower colony-forming units per milliliter than the control. To explore the underlying mechanisms of this phenomenon in CRC cells, we determined the targets of significant differential gene expression which are related to the malignancy of cancer and found a significant decrease in c-Met, MMPs, and cyclinD1 expression in MC-38 cells (**Figure 6C**). Similarly, the YYFZBJS-primed BMDMs could also suppress the infiltration ability of the tumor cells (**Figure 6D**). Based on the RNA sequencing in previous results, the noticeable changes of mRNA were further analyzed by PCR in MC-38 cells co-cultured with YYFZBJS-primed BMDMs (**Figure 6E**). Interestingly, we found that YYFZBJS primed BMDMs could significantly decrease the phosphorylation of STAT3, while BMDMs from C57 mice could effectively increase the level of STAT3 and p-STAT3 (**Figure 6F**).

Discussion

Epidemiologic studies suggest that herbal medicines can reduce colon cancer risk in humans [35]. Studies have previously revealed the anti-tumor effect of YYFZBJS and its modulating effect in the gut microbiome and its role in delaying colonic tumorigenesis progression [5]. Several recent studies have confirmed the link between gut microbiome dysbiosis and colorectal cancer [36, 37]. However, no studies investigating the impact of TCM on the balance between the gut microbiome and immune cells in the colonic tumorigenesis have been reported.

Here, we showed that YYFZBJS, a traditional Chinese herbal medicine from Synopsis of Golden Chamber, significantly reduced tumor multiplicity and numbers in the AOM/DSS mouse model. This is in line with previous studies in *Apc*$^{Min/+}$ mice where YYFZBJS FMT administration was shown to influence microbial consortium in colorectal carcinogenesis and significantly reduced overall polyp number size. In the present study, OTUs results further showed that *Bacteroidetes*, *Ruminococcaceae*, and *Lactobacillus*, might play an active role in both the pro-inflammatory and anti-inflammatory macrophages regulatory pathways. Interestingly, several studies have highlighted that induced colon macrophages are closely related to the gut microbiome and play roles in promoting tumor function [38, 39]. Recently, some studies have reported that the intestinal flora can activate intestinal mucosal cells through mucosal macrophages, triggering innate immune responses and producing marginal effects, thereby promoting the occurrence and development of CRC [40].

To our knowledge, pathogenic bacteria can stimulate infection, inflammation, and carcinogenesis, whereas the relationship between IBD and CRC is well established [41]. Notably, the enterotoxigenic B. fragilis (ETBF) forms a biofilm, produces toxins, and plays an important role in promoting CRC, whereas the nontoxigenic Bacteroides fragilis (NTBF) plays a beneficial role in many diseases. In the current study, our data uncovered that ETBF administration modulated the microbial consortia in colorectal carcinogenesis and significantly increased the overall tumor number and size. Furthermore, we confirmed that ETBF promoted the M2 polarization of macrophages to promote tumor growth, resulting in the occurrence and progression of CRC. Other studies and ours have also shown that M2 macrophages can promote colorectal cancer metastasis via M2 macrophage-secreted protein and/or regulatory factors [17, 42].

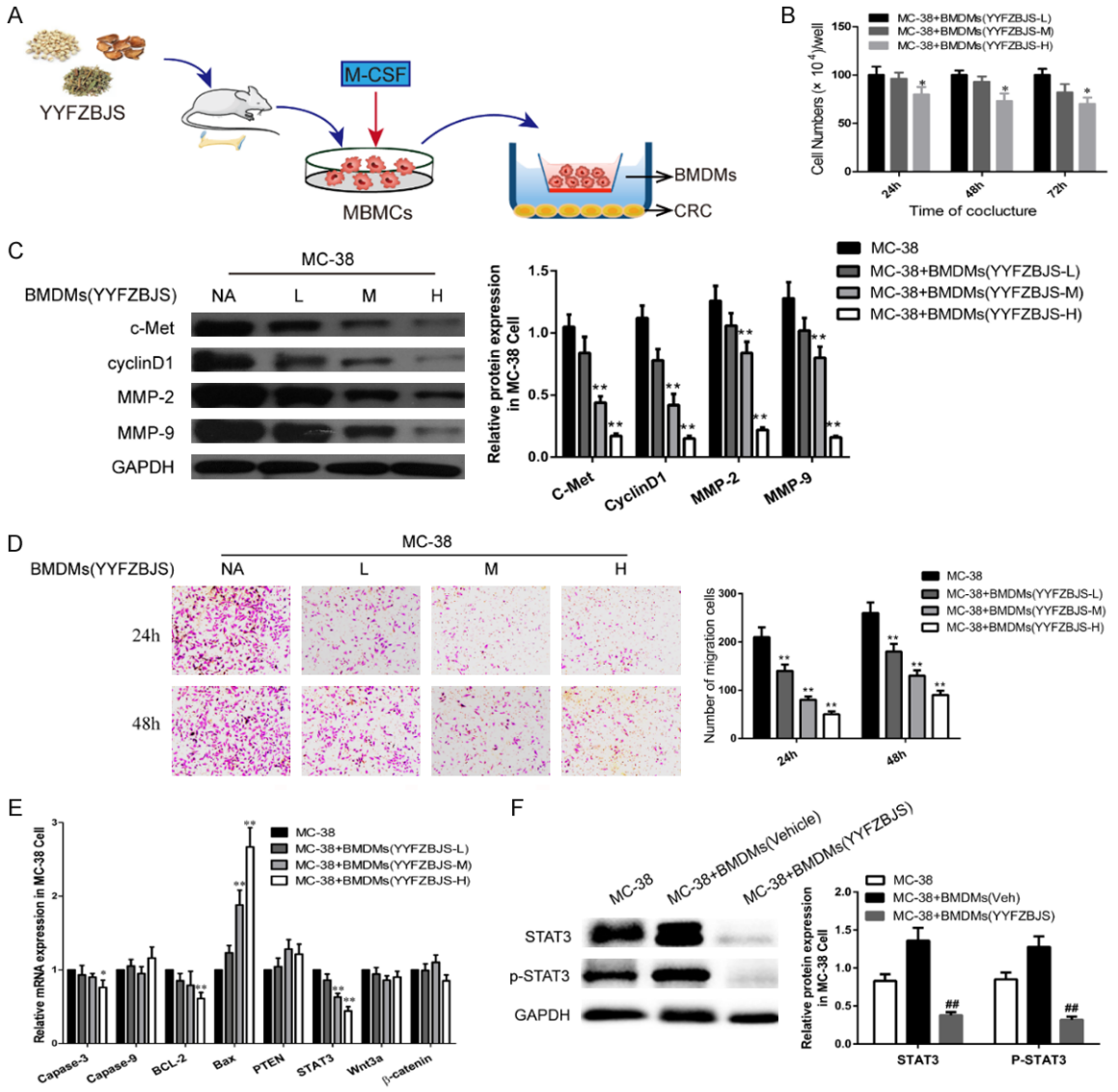

Figure 6. YYFZBJS inhibited tumor cell proliferation through regulating ETBF primed BMDMs *in vitro*. A. Experimental design indicating bone marrow-derived macrophages (BMDMs) were isolated from the bone marrow of C57BL/6J mice treated with or without YYFSBJS at the doses of 3.825 g/kg, 7.65 g/kg and 15.3 g/kg for 2 weeks. The BMDMs were from femurs and tibias of mice and cultured in a special medium (DMEM containing 10% FBS supplemented with 50 μg/ml penicillin/streptomycin and 10 ng/ml recombinant macrophage colony-stimulating factor [M-CSF; Thermo Fisher Scientific]). Then the primed BMDMs (TAM) were collected and were assigned to MC-38 cells in a 10:1 ratio. B. MC-38 cells proliferation was assayed at 24, 48, and 72 h after co-culture with the M2φ. The data are presented as the mean ± SD from at least three experiments. $^{*}P<0.05$, $^{**}P<0.01$ *vs.* MC-38+BMDMs (YYFZBJS-L). C, F. Western blot and quantitative assay of c-Met, cyclinD1, MMP-2, MMP-9, STAT3 and phosphorylation of STAT3 in MC-38 cells. GAPDH is the loading control. The data are presented as the mean ± SD from at least three independent experiments. $^{**}P<0.01$ *vs.* MC-38; $^{\#}P<0.05$, $^{\#\#}P<0.01$ *vs.* MC-38+TAM (Veh). D. Cell invasion assay result using Matrigel-coated Transwell. (left, representative pictures of invasion chambers; right, average counts from five random microscopic fields). Data are presented as mean ± SD of triplicate experiments. $^{**}P < 0.01$ *vs.* MC-38. E. mRNA expression of genes associated with cell proliferation in MC-38 cells was evaluated using quantitative RT-PCR. The data are presented as the mean ± SD from at least three experiments. $^{*}P<0.05$, $^{**}P<0.01$ *vs.* MC-38.

In addition, ETBF infection-mediated tumorigenesis is contributed by STAT3 signaling of Th17 cells or colon epithelial cells in a spontaneous intestinal tumor model [43]. Specifically, ETBF has the ability to activate STAT3 rapidly in both colonic epithelial cells and colonic mucosal immune cells through phosphorylation and nuclear translocation. Similar to our in vitro results, our microarray data suggest that ETBF-primed macrophages can facilitate

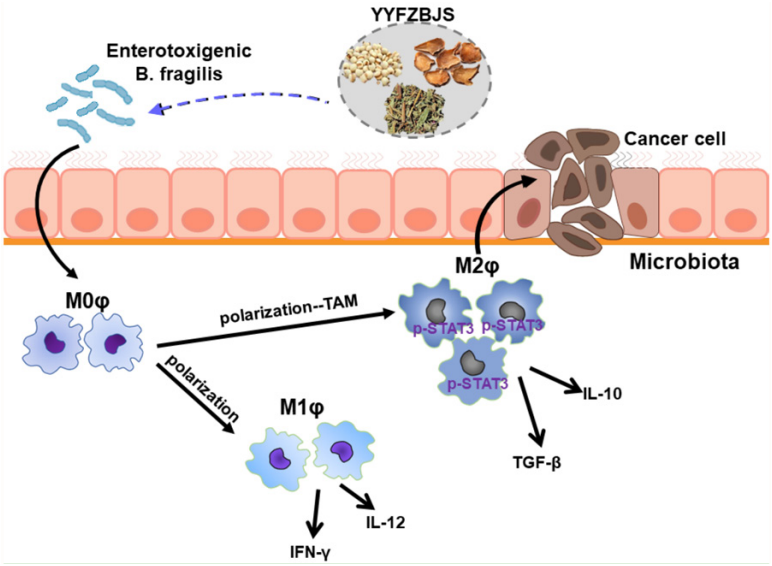

Figure 7. A schematic of the effect of YYFZBJS in host-microbiota interactions in colorectal cancer prevention.

tumor cell proliferation and oncogenic pathways in CRC carcinogenesis, particularly the STAT3, JNK, and NF-κB signaling pathway, because of the significant impacts on M2 macrophage polarization.

Accumulating data also indicate that the percentage of M2 macrophage is inversely related to an increased risk of cancer progression [44, 45]. CRC patients often show aberrantly high levels of M2 macrophage in peripheral blood, tumor-draining lymph node (DLN), and tumor microenvironment [46]. Coincidently, M2 macrophages have also been reported by clinical observations and mechanistic studies to play an indispensable role as a promoter of tumor growth because of its suppressive effects on the autologous effector T-cell responses. Our previous study noted that M2 phenotype macrophages, in particular, seemed to promote tumor malignant transformation of the AOM/DSS mice model due to the presence of the up-regulation of CD206, Arg-1, IL-10, and TGF-β, which are the primary M2 markers [17]. The current study also found that ETBF infection increases IL-6, IL-10, and TGF-β in the peripheral blood of AOM/DSS mouse models and Arg-1 expression in ETBF primed macrophages. Take together, our results revealed that ETBF could provide the required impetus in M2-macrophage-mediated tumorigenesis.

To explore the anti-tumor mechanism of YYFZBJS in the gut microbiome, we are first to show the effect of co-culturing tumor cells and BMDMs derived from YYFZBJS treated mice (**Figure 6A**). Interestingly, YYFZBJS primed macrophages showed insignificant changes in the cell viability of CRC MC-38 cells in a time and dose-dependent manner. Our results also show that in supernatants of cultured tumor cells, the tumorigenic correlation genes, protein and phosphorylation of protein such as STAT3 in CRC cells were suppressed by the YYFZBJS primed macrophages, indicating that YYFZBJS primarily inhibits the STAT3, JNK, and NF-κB signaling pathways. Moreover, our results indicate that YYFZBJS indirectly inhibited colon cell proliferation and altered the differentiation of the M2 phenotype in the co-culture microenvironment, suggesting that the role of TAMs in promoting tumor growth can be reduced by YYFZBJS (**Figure 7**).

In summary, we demonstrate that YYFZBJS prevents colon tumorigenesis using an AOM/DSS mouse model. The ETBF mediated the anti-tumor effect for promoting macrophage polarization, leading to the phosphorylation of STAT3 and proliferation of tumor cells. Specifically, we demonstrate that ETBF can influence the growth of cancer cells via BMDMs from YYFZBJS treated mice. These findings suggest potential new mechanisms by which TCM can prevent colitis-associated tumorigenesis by inhibiting commensal microbiota via M2 macrophage polarization. This discovery helps us better understand the anticancer effect of YYFZBJS and its ability to remodel the gut microbiota, leading to regulation of immunity and delay of carcinogenesis.

Acknowledgements

The authors thank Dr. Lu Zhang for the data from the analysis of fecal flora. This research was supported by the Science Foundation for

Shanghai Committee of Science Project (No. 21S21901400, 21010504300), the Project of Shanghai Municipal Health Commission (No. 20204Y0401), the Project of Shanghai University of Traditional Chinese Medicine (No. 2019LK009).

Disclosure of conflict of interest

None.

Abbreviations

CRC, Colorectal cancer; ETBF, Bacteroides fragilis; GF, germ free; YYFZBJS, Yi-Yi-Fu-Zi-Bai-Jiang-San; DAI, disease activity index; AOM, azoxymethane/dextran sulfate sodium, AOM/DSS; TAMs, tumor-associated macrophages; ACF, aberrant crypt foci; PCNA, Proliferating Cell Nuclear Antigen; IFN-γ, interferon gamma; IL-4/6/10, interleukin-4/6/10; TNF-α, tumor necrosis factor-α; Apc, adenomatous polyposis coli; PBS, Phosphate-buffered saline; TCM, Traditional Chinese Medicine; IHC, Immunohistochemistry; qRT-PCR, real time quantitative reverse transcription PCR.

Address correspondence to: Dr. Hua Sui, Medical Experiment Center, Jiading Branch of Shanghai General Hospital, Shanghai Jiao Tong University School of Medicine, 800 Huangjiahuayuan Road, Shanghai 201803, China. Tel: +86-21-67339339; E-mail: syh0808@163.com; Dr. Huirong Zhu, Shanghai University of Traditional Chinese Medicine, 1200 Cailun Road, Shanghai 201203, China. Tel: +86-18916003000; E-mail: huirong_zhu@126.com

References

[1] Lee YK, Mehrabian P, Boyajian S, Wu WL, Selicha J, Vonderfecht S and Mazmanian SK. The protective role of bacteroides fragilis in a murine model of colitis-associated colorectal cancer. mSphere 2018; 3: e00587-18.

[2] Hwang S, Jo M, Hong JE, Park CO, Lee CG and Rhee KJ. Protective effects of zerumbone on colonic tumorigenesis in enterotoxigenic bacteroides fragilis (ETBF)-colonized AOM/DSS BALB/c mice. Int J Mol Sci 2020; 21: 857.

[3] Gopalakrishnan V, Helmink BA, Spencer CN, Reuben A and Wargo JA. The influence of the gut microbiome on cancer, immunity, and cancer immunotherapy. Cancer Cell 2018; 33: 570-580.

[4] Si H, Yang Q, Hu H, Ding C, Wang H and Lin X. Colorectal cancer occurrence and treatment based on changes in intestinal flora. Semin Cancer Biol 2021; 70: 3-10.

[5] Sui H, Zhang L, Gu K, Chai N, Ji Q, Zhou L, Wang Y, Ren J, Yang L, Zhang B, Hu J and Li Q. YYFZBJS ameliorates colorectal cancer progression in Apc(Min/+) mice by remodeling gut microbiota and inhibiting regulatory T-cell generation. Cell Commun Signal 2020; 18: 113.

[6] Cao Y, Wang Z, Yan Y, Ji L, He J, Xuan B, Shen C, Ma Y, Jiang S, Ma D, Tong T, Zhang X, Gao Z, Zhu X, Fang J, Chen H and Hong J. Enterotoxigenic bacteroides fragilis promotes intestinal inflammation and malignancy by inhibiting exosomes-packaged miR-149-3p. Gastroenterology 2021; [Epub ahead of print].

[7] Boleij A, Hechenbleikner EM, Goodwin AC, Badani R, Stein EM, Lazarev MG, Ellis B, Carroll KC, Albesiano E, Wick EC, Platz EA, Pardoll DM and Sears CL. The bacteroides fragilis toxin gene is prevalent in the colon mucosa of colorectal cancer patients. Clin Infect Dis 2015; 60: 208-215.

[8] Sears CL, Islam S, Saha A, Arjumand M, Alam NH, Faruque AS, Salam MA, Shin J, Hecht D, Weintraub A, Sack RB and Qadri F. Association of enterotoxigenic bacteroides fragilis infection with inflammatory diarrhea. Clin Infect Dis 2008; 47: 797-803.

[9] Dejea CM, Fathi P, Craig JM, Boleij A, Taddese R, Geis AL, Wu X, DeStefano Shields CE, Hechenbleikner EM, Huso DL, Anders RA, Giardiello FM, Wick EC, Wang H, Wu S, Pardoll DM, Housseau F and Sears CL. Patients with familial adenomatous polyposis harbor colonic biofilms containing tumorigenic bacteria. Science 2018; 359: 592-597.

[10] Gu T, Li Q and Egilmez NK. IFNβ-producing CX-3CR1(+) macrophages promote T-regulatory cell expansion and tumor growth in the APC(min/+)/bacteroides fragilis colon cancer model. Oncoimmunology 2019; 8: e1665975.

[11] Verma S, Prescott R and Cherayil BJ. The commensal bacterium bacteroides fragilis downregulates ferroportin expression and alters iron homeostasis in macrophages. J Leukoc Biol 2019; 106: 1079-1088.

[12] Geis AL, Fan H, Wu X, Wu S, Huso DL, Wolfe JL, Sears CL, Pardoll DM and Housseau F. Regulatory T-cell response to enterotoxigenic bacteroides fragilis colonization triggers IL17-dependent colon carcinogenesis. Cancer Discov 2015; 5: 1098-1109.

[13] Gu T, De Jesus M, Gallagher HC, Burris TP and Egilmez NK. Oral IL-10 suppresses colon carcinogenesis via elimination of pathogenicCD4(+) T-cells and induction of antitumor CD8(+) T-cell activity. Oncoimmunology 2017; 6: e1319027.

[14] Malik A, Sharma D, Malireddi RKS, Guy CS, Chang TC, Olsen SR, Neale G, Vogel P and Kanneganti TD. SYK-CARD9 signaling axis promotes gut fungi-mediated inflammasome acti-

vation to restrict colitis and colon cancer. Immunity 2018; 49: 515-530, e5.
[15] Davis TA, Conradie D, Shridas P, de Beer FC, Engelbrecht AM and de Villiers WJS. Serum amyloid A promotes inflammation-associated damage and tumorigenesis in a mouse model of colitis-associated cancer. Cell Mol Gastroenterol Hepatol 2021; 12: 1329-1341.
[16] DeNardo DG and Ruffell B. Macrophages as regulators of tumour immunity and immunotherapy. Nat Rev Immunol 2019; 19: 369-382.
[17] Sui H, Tan H, Fu J, Song Q, Jia R, Han L, Lv Y, Zhang H, Zheng D, Dong L, Wang S, Li Q and Xu H. The active fraction of garcinia yunnanensis suppresses the progression of colorectal carcinoma by interfering with tumorassociated macrophage-associated M2 macrophage polarization in vivo and in vitro. FASEB J 2020; 34: 7387-7403.
[18] Yahaya MAF, Lila MAM, Ismail S, Zainol M and Afizan NARNM. Tumour-associated macrophages (TAMs) in colon cancer and how to reeducate them. J Immunol Res 2019; 2019: 2368249.
[19] Tan SY, Fan Y, Luo HS, Shen ZX, Guo Y and Zhao LJ. Prognostic significance of cell infiltrations of immunosurveillance in colorectal cancer. World J Gastroenterol 2005; 11: 1210-1214.
[20] Cui YL, Li HK, Zhou HY, Zhang T and Li Q. Correlations of tumor-associated macrophage subtypes with liver metastases of colorectal cancer. Asian Pac J Cancer Prev 2013; 14: 1003-1007.
[21] Jayme TS, Leung G, Wang A, Workentine ML, Rajeev S, Shute A, Callejas BE, Mancini N, Beck PL, Panaccione R and McKay DM. Human interleukin-4-treated regulatory macrophages promote epithelial wound healing and reduce colitis in a mouse model. Sci Adv 2020; 6: eaba4376.
[22] Tilg H, Adolph TE, Gerner RR and Moschen AR. The intestinal microbiota in colorectal cancer. Cancer Cell 2018; 33: 954-964.
[23] Dumitrescu O, Choudhury P, Boisset S, Badiou C, Bes M, Benito Y, Wolz C, Vandenesch F, Etienne J, Cheung AL, Bowden MG and Lina G. Beta-lactams interfering with PBP1 induce panton-valentine leukocidin expression by triggering sarA and rot global regulators of staphylococcus aureus. Antimicrob Agents Chemother 2011; 55: 3261-3271.
[24] Fessler J, Matson V and Gajewski TF. Exploring the emerging role of the microbiome in cancer immunotherapy. J Immunother Cancer 2019; 7: 108.
[25] Missiaglia E, Jacobs B, D'Ario G, Di Narzo AF, Soneson C, Budinska E, Popovici V, Vecchione L, Gerster S, Yan P, Roth AD, Klingbiel D, Bosman FT, Delorenzi M and Tejpar S. Distal and proximal colon cancers differ in terms of molecular, pathological, and clinical features. Ann Oncol 2014; 25: 1995-2001.
[26] van Leeuwen BL, Påhlman L, Gunnarsson U, Sjövall A and Martling A. The effect of age and gender on outcome after treatment for colon carcinoma. A population-based study in the Uppsala and Stockholm region. Crit Rev Oncol Hematol 2008; 67: 229-236.
[27] Zheng YY, Viswanathan B, Kesarwani P and Mehrotra S. Dietary agents in cancer prevention: an immunological perspective. Photochem Photobiol 2012; 88: 1083-1098.
[28] Ying W, Riopel M, Bandyopadhyay G, Dong Y, Birmingham A, Seo JB, Ofrecio JM, Wollam J, Hernandez-Carretero A, Fu W, Li P and Olefsky JM. Adipose tissue macrophage-derived exosomal mirnas can modulate in vivo and in vitro insulin sensitivity. Cell 2017; 171: 372-384, e312.
[29] Sui H, Liu X, Jin BH, Pan SF, Zhou LH, Yu NA, Wu J, Cai JF, Fan ZZ, Zhu HR and Li Q. Zuo Jin Wan, a traditional Chinese herbal formula, reverses P-gp-mediated MDR in vitro and in vivo. Evid Based Complement Alternat Med 2013; 2013: 957078.
[30] Hwang S, Jo M, Hong JE, Park CO, Lee CG, Yun M and Rhee KJ. Zerumbone suppresses enterotoxigenic bacteroides fragilis infection-induced colonic inflammation through inhibition of NF-κB. Int J Mol Sci 2019; 20: 4560.
[31] Li R, Zhou R, Wang H, Li W, Pan M, Yao X, Zhan W, Yang S, Xu L, Ding Y and Zhao L. Gut microbiota-stimulated cathepsin K secretion mediates TLR4-dependent M2 macrophage polarization and promotes tumor metastasis in colorectal cancer. Cell Death Differ 2019; 26: 2447-2463.
[32] Jaeckel S, Kaller M, Jackstadt R, Götz U, Müller S, Boos S, Horst D, Jung P and Hermeking H. Ap4 is rate limiting for intestinal tumor formation by controlling the homeostasis of intestinal stem cells. Nat Commun 2018; 9: 3573.
[33] Sui H, Xu H, Ji Q, Liu X, Zhou L, Song H, Zhou X, Xu Y, Chen Z, Cai J, Ji G and Li Q. 5-hydroxytryptamine receptor (5-HT1DR) promotes colorectal cancer metastasis by regulating Axin1/β-catenin/MMP-7 signaling pathway. Oncotarget 2015; 6: 25975-25987.
[34] Sui H, Zhao J, Zhou L, Wen H, Deng W, Li C, Ji Q, Liu X, Feng Y, Chai N, Zhang Q, Cai J and Li Q. Tanshinone IIA inhibits β-catenin/VEGF-mediated angiogenesis by targeting TGF-β1 in normoxic and HIF-1α in hypoxic microenvironments in human colorectal cancer. Cancer Lett 2017; 403: 86-97.
[35] Ji Q, Zhou L, Sui H, Yang L, Wu X, Song Q, Jia R, Li R, Sun J, Wang Z, Liu N, Feng Y, Sun X, Cai G, Feng Y, Cai J, Cao Y, Cai G, Wang Y and Li Q. Primary tumors release ITGBL1-rich extracel-

lular vesicles to promote distal metastatic tumor growth through fibroblast-niche formation. Nat Commun 2020; 11: 1211.
[36] Long X, Wong CC, Tong L, Chu ESH, Ho Szeto C, Go MYY, Coker OO, Chan AWH, Chan FKL, Sung JJY and Yu J. Peptostreptococcus anaerobius promotes colorectal carcinogenesis and modulates tumour immunity. Nat Microbiol 2019; 4: 2319-2330.
[37] Li H, Xu F, Li S, Zhong A, Meng X and Lai M. The tumor microenvironment: an irreplaceable element of tumor budding and epithelial-mesenchymal transition-mediated cancer metastasis. Cell Adh Migr 2016; 10: 434-446.
[38] Colby JK, Jaoude J, Liu F and Shureiqi I. Oxygenated lipid signaling in tumor-associated macrophages-focus on colon cancer. Cancer Metastasis Rev 2018; 37: 289-315.
[39] Kay C, Wang R, Kirkby M and Man SM. Molecular mechanisms activating the NAIP-NLRC4 inflammasome: implications in infectious disease, autoinflammation, and cancer. Immunol Rev 2020; 297: 67-82.
[40] Grivennikov SI, Wang K, Mucida D, Stewart CA, Schnabl B, Jauch D, Taniguchi K, Yu GY, Osterreicher CH, Hung KE, Datz C, Feng Y, Fearon ER, Oukka M, Tessarollo L, Coppola V, Yarovinsky F, Cheroutre H, Eckmann L, Trinchieri G and Karin M. Adenoma-linked barrier defects and microbial products drive IL-23/IL-17-mediated tumour growth. Nature 2012; 491: 254-258.
[41] Cho M, Carter J, Harari S and Pei Z. The interrelationships of the gut microbiome and inflammation in colorectal carcinogenesis. Clin Lab Med 2014; 34: 699-710.
[42] Ha CWY, Martin A, Sepich-Poore GD, Shi B, Wang Y, Gouin K, Humphrey G, Sanders K, Ratnayake Y, Chan KSL, Hendrick G, Caldera JR, Arias C, Moskowitz JE, Ho Sui SJ, Yang S, Underhill D, Brady MJ, Knott S, Kaihara K, Steinbaugh MJ, Li H, McGovern DPB, Knight R, Fleshner P and Devkota S. Translocation of viable gut microbiota to mesenteric adipose drives formation of creeping fat in humans. Cell 2020; 183: 666-683, e617.
[43] Chung L, Thiele Orberg E, Geis AL, Chan JL, Fu K, DeStefano Shields CE, Dejea CM, Fathi P, Chen J, Finard BB, Tam AJ, McAllister F, Fan H, Wu X, Ganguly S, Lebid A, Metz P, Van Meerbeke SW, Huso DL, Wick EC, Pardoll DM, Wan F, Wu S, Sears CL and Housseau F. Bacteroides fragilis toxin coordinates a pro-carcinogenic inflammatory cascade via targeting of colonic epithelial cells. Cell Host Microbe 2018; 23: 203-214, e205.
[44] Yang Y, Li L, Xu C, Wang Y, Wang Z, Chen M, Jiang Z, Pan J, Yang C, Li X, Song K, Yan J, Xie W, Wu X, Chen Z, Yuan Y, Zheng S, Yan J, Huang J and Qiu F. Cross-talk between the gut microbiota and monocyte-like macrophages mediates an inflammatory response to promote colitis-associated tumourigenesis. Gut 2020; 70: 1495-1506.
[45] Xia Y, Rao L, Yao H, Wang Z, Ning P and Chen X. Engineering macrophages for cancer immunotherapy and drug delivery. Adv Mater 2020; 32: e2002054.
[46] Aalipour A, Chuang HY, Murty S, D'Souza AL, Park SM, Gulati GS, Patel CB, Beinat C, Simonetta F, Martinić I, Gowrishankar G, Robinson ER, Aalipour E, Zhian Z and Gambhir SS. Engineered immune cells as highly sensitive cancer diagnostics. Nat Biotechnol 2019; 37: 531-539.

Supplementary Material

Quantitative real-time PCR

RNA was isolated from colon tissues or cells by TRIzol (Invitrogen) and reverse-transcribed into cDNA by PrimeScript RT Master Mix (#A360, TaKaRa). qPCR was performed by Quantitative RT-PCR (ABI-7300). The relative expression of target gene was calculated using the $2^{\Delta}C_{(t)}$ method. Fold change of target gene expression were calculated by normalization to control group. The primer sequences are shown in Tables S2 and S3.

References

[1] Chen J, Jayachandran M, Zhang W, Chen L, Du B, Yu Z and Xu B. Dietary supplementation with sea bass (lateolabrax maculatus) ameliorates ulcerative colitis and inflammation in macrophages through inhibiting toll-like receptor 4-linked pathways. Int J Mol Sci 2019; 20: 2907.

[2] Sui H, Zhang L, Gu K, Chai N, Ji Q, Zhou L, Wang Y, Ren J, Yang L, Zhang B, Hu J and Li Q. YYFZBJS ameliorates colorectal cancer progression in *Apc*$^{Min/+}$ mice by remodeling gut microbiota and inhibiting regulatory T-cell generation. Cell Commun Signal 2020; 18: 113.

Table S1. DAI score in C57 mice (at the end of experiment)

Group	Symptom score			Disease activity index (DAI)
	weight loss	stool consistency	occult blood	
Control	2.625	2.75	2.25	2.54
YYFZBJS-L	2.5	2.25	1.5	2.08
YYFZBJS-M	2.75	2	0.75	1.83
YYFZBJS-H	3	1.25	0.5	1.58
Aspirin	2.875	1.25	0.5	1.54

Symptom score including weight loss score, stool consistency score and occult blood score. The evaluation criterion of Symptom score was described as previous [1]. DAI = (weight loss score + stool consistency score + occult blood score)/3.

Table S2. PCR primers

gene	Forward primer	Reverse primer
Clostridium butyricum	CCTCCTTTCTATGGAGAAATCTAGCA	TGTAGCTTGACCTTTTTAAGTTTTGA
Akkermansia	CAGCACGTGAAGGTGGGGAC	CCTTGCGGTTGGCTTCAG
Enterotoxigenic B. fragilis	GGGACAAGGATTCTACCAGCTTTATA	ATTCGGCAATCTCATTCATCATT
Lactobacillus rhamnosus	TGCATCTTGATTTAATTTTG	CCCACTGC TGCCTCCCGTAGGAGT

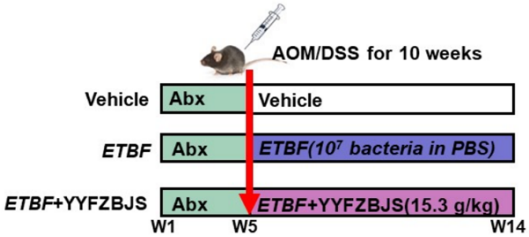

Figure S1. Experimental design indicating the timing of the intragastric administration and organization of groups. Mice were treated with Abx from W1 (age at week 4) to W4, then injected with AOM (12.5 mg/kg, i.p.) and provided drinking water for 1 week, and three cycles with DSS and drinking water for 3 weeks as described in the Methods section. During the treatment, Vehicle, ETBF and YYFZBJS were oral administration with 10^8 CFU/mice. The intragastric administration of YYFZBJS was taken at the doses of 15.3 g/kg with the high dose according to HED (human equivalent dose) as previous [2].

Table S3. PCR primers

gene	Forward primer	Reverse primer
CD30L	AAGTTTGCCTGGGTCCTCTC	CCACTCCCAATCATGTGGCT
CD54	AGTCGTCCGCTTCCGCTACC	AGGGTGAGGTCCTTGCCTACTTG
IL-1α	CATTGGCGTTTGAGTCAGCA	CATGGAGTGGGCCATAGCTT
CXCL-1	AACATGCCAGCCACTGTGAT	GCCCCTTTGTTCTAAGCCAG
GM-CSF	ACCCGCTCACCCATCACTGTC	GGCATGTCATCCAGGAGGTTCAG
CCL12	AGCTACCACCATCAGTCCTCAGG	ACACTGGCTGCTTGTGATTCTCC
IL-13	CTCTTGCTTGCCTTGGTGGTCTC	TTGTGTGATGTTGCTCAGCTCCTC
Leptin	GGTTCCTGTGGCTTTGGTCCTATC	ACCCTCTGCTTGGCGGATACC
TIMP-1	AGGATTCAAGGCTGTGGGAAATGC	CTTCACTGCGGTTCTGGGACTTG
IL-10	TGAAAACAAGAGCAAGGCCG	GCCACCCTGATGTCTCAGTT
IL-4	TCTTTGCTGCCTCCAAGAACA	GTTCCTGTCGAGCCGTTTCA
IL-6	CCACCGGGAACGAAAGAGAA	TCTTCTCCTGGGGGTACTGG
IFNα	CCTGATGAATGCGGACTCCA	TAGCAGGGGTGAGAGTCTTTG
TNFα	CATCTTCTCAAAATTCGAGTGACAA	TGGGAGTAGACAAGGTACAACCC
MMP1	AGAAAGAAGACAAAGGCAAGTTGA	TTCCCAGTCACTTTCAGCCC
MMP9	TCTATGGTCCTCGCCCTGAA	CATCGTCCACCGGACTCAAA
Bax	CATGGGCTGGACATTGGACT	AAAGTAGGAGAGGAGGCCGT
BCL-2	CTTTGAGTTCGGTGGGGTCA	GGGCCGTACAGTTCCACAAA
PTEN	GGAAAGGGACGGACTGGTGTAATG	CGCCTCTGACTGGGAATTGTGAC
STAT3	AATCTCAACTTCAGACCCGCCAAC	GCTCCACGATCCTCTCCTCCAG
Wnt3a	TGCCGATGCCAGGGAGAACC	CCAGCAGGTCTTCACTTCACAGC
β-catenin	TGCCGTTCGCCTTCATTATGGAC	TGGGCAAAGGGCAAGGTTTCG
GAPDH	TGTGTCCGTCGTGGATCTGA	CCTGCTTCACCACCTTCTTGA